

A density functional study of inhibition of the HDS hydrogenation pathway by pyridine, benzene, and H₂S on MoS₂-based catalysts

Áshildur Logadóttir^a, Poul Georg Moses^b, Berit Hinnemann^b, Nan-Yu Topsøe^a,
Kim G. Knudsen^a, Henrik Topsøe^{a,**}, Jens K. Nørskov^{b,*}

^a Haldor Topsøe A/S, Nymøllevej 55, DK-2800 Lyngby, Denmark

^b Center for Atomic-scale Materials Physics (CAMP), Nano DTU, Department of Physics, Building 307,
Technical University of Denmark, DK-2800 Lyngby, Denmark

Available online 28 November 2005

Abstract

The inhibition of catalytic hydrodesulfurization (HDS) by basic nitrogen compounds is an important problem in the production of ultra low sulfur transportation fuels and the origin of the inhibition effects is presently elucidated by performing density functional theory (DFT) calculations on the interaction of pyridine with the two types of edges of MoS₂ catalyst nanoparticles. Particular attention is given to studies of the hydrogenation (HYD) pathway in HDS since this is the favored pathway for refractory sulfur compounds and it is the pathway, which is most severely poisoned by basic nitrogen compounds. In order to understand the observed inhibitor trends, DFT studies on the adsorption of benzene, which is a weaker poison than pyridine, and H₂S, which has no or only a very minor influence on the HYD pathway, have also been made. We find that the adsorption of pyridine is quite strong and especially strong at positions along the so-called Mo edge. Thus, the HYD reaction most likely involves sites at this edge. This suggestion is substantiated by the observation that the adsorption blocks the metallic like so-called brim sites, which were recently shown to be involved in the HYD pathway. Furthermore, H₂S is observed not to interact strongly with these sites. The present results have also provided insight into the nitrogen compound inhibition of the direct desulfurization DDS pathway. The difference in the poisoning by benzene and pyridine is observed to be related to the ease with which hydrogen from neighboring SH group can be transferred to the pyridine molecule resulting in the creation of more strongly held pyridinium ions. At the so-called S edge, hydrogen is tightly bound and this transfer is not favored. The present results, therefore, also stress the importance of the hydrogen binding properties of HDS catalysts.

© 2005 Elsevier B.V. All rights reserved.

Keywords: Hydrodesulfurization; Hydrogenation; Inhibition; DFT; Brim sites; Brønsted acid sites; MoS₂; Pyridine; Benzene; H₂S

1. Introduction

It has been known for many years that dibenzothiophene (DBT) may be desulfurized by two different reaction pathways, i.e., the direct desulfurization (DDS) pathway and the hydrogenation (HYD) pathway [1]. Early studies [2] also showed that the presence of alkyl groups on the DBT skeleton might reduce the reactivity, especially if the substituents are located close to the sulfur like in the case of 4,6-dimethyldibenzothiophene (4,6-DMDBT). Recently, there

has been a worldwide demand for producing transportation fuels with ultra low sulfur contents [3–12] and real feed studies have shown that this requires the removal of refractory compounds like 4,6-DMDBT. Model compound studies have shown that the HDS reaction for the unsubstituted DBT molecule proceeds mainly via the direct (DDS) route [1,7,13]. However, in the case of sterically hindered alkyl substituted molecules like 4,6-DMDBT, the rate for the DDS route is diminished whereas the rate for sulfur removal via the prehydrogenation HYD route may remain relatively unaffected [7]. Thus, for HDS of sterically hindered molecules the HYD route may become very important [5,7–9,13–18].

In real feed operation, the extent to which a given catalyst desulfurizes via one route or the other will depend on the hydrogen and H₂S partial pressures, on the conversion, and on the properties of the feed [9,17]. Many of these effects appear to

* Corresponding author. Tel.: +45 4525 3175; fax: +45 4593 2399.

** Corresponding author. Tel.: +45 4527 2000; fax: +45 4527 2999.

E-mail addresses: het@topsoe.dk (H. Topsøe), norskov@fysik.dtu.dk (J.K. Nørskov).

be related to the fact that different molecules in the feed may have quite different inhibiting effects on the two reaction routes. The presence of nitrogen compounds is, for example, a key parameter, which may influence the HDS activity [11,13,17–28]. Recent detailed studies of inhibition effects under real feed conditions [22] showed that it is especially basic heterocyclic nitrogen compounds that inhibit the HDS reaction and the inhibition is most pronounced for the HYD route. Thus, the inhibition effects are particular important for deep HDS of refractory compounds. Kinetic studies using model compounds also support this conclusion [24,29]. For non-sterically hindered heterocyclic compounds with nitrogen in a six-membered ring, there appears to be a good correlation between the inhibitor strength and the gas phase proton affinities, where stronger inhibitors have higher gas phase proton affinity [20,21]. This could indicate that the poisoning of the HYD route by nitrogen compounds involves the interaction with a proton from a Brønsted acid site on the catalytically active nanostructures. Infrared measurements have shown that SH groups exist at the edges of MoS₂ nanoparticles [29] and IR studies have also revealed their interaction with pyridine to form pyridinium ions [30]. The inhibiting effect of other molecules on the HYD route has also been investigated. Aromatic hydrocarbons have been observed to poison the HYD route more than the DDS route [13,18,31,32] but for real-life operating conditions, the poisoning effect on HYD may be quite small [17,24]. In contrast, the H₂S inhibiting effect is much less for HYD than for DDS [13,17,33]. Recently, it was found that the H₂S inhibition of the HYD route could be related to the poisoning of the final hydrogenolysis step of this route (which is similar to DDS) and not to poisoning of the preceding hydrogenation steps [16].

While there is a quite good general agreement in the literature on the different reactivity, kinetic and poisoning effects, very limited direct mechanistic insight has resulted. Nevertheless, many of the above-mentioned observations have been taken as evidence for the HYD and DDS pathways occurring on different sites [13,16,34]. Sulfur vacancies are in general believed to play a key role in the DDS pathway. The nature of the hydrogenation sites is less well understood but many authors have also proposed vacancies to be involved in HYD reactions (see e.g. [13]). In view of the observation that quite large molecules may be desulfurized via the HYD pathway it has been proposed that multiple vacancy sites or ensembles of vacancies are involved in HYD. It has, for example, been suggested [35] that the HYD reaction occurs at the so-called naked MoS₂ edge (i.e. the 10 $\bar{1}$ 0 Mo edge without terminal sulfur atoms). Many DFT studies [36–40] have used the naked Mo edge as a starting point for addressing mechanistic issues. However, recent results have shown that it is energetically extremely unfavorable to create such naked Mo edges [41,42]. The edges bind sulfur very strongly and naked edges will not be present under realistic reaction conditions. The observation that the HYD reaction is not strongly inhibited by H₂S also allows one to exclude that naked Mo edges can play an important role in hydrotreating.

Recently, it has been possible to obtain important clues about the HYD pathway since atomically resolved scanning

tunneling microscopy (STM) images could be obtained of key intermediates of this path [43]. DFT calculations provided detailed insight into the origin of the observations and the reaction was shown to involve metallic edge states (the so-called brim sites) located slightly inside the MoS₂ nanoparticles adjacent to the Mo edge itself.

Several DFT studies have investigated the equilibrium edge configuration of MoS₂ [41,42,44]. These studies have led to the construction of phase diagrams of edge configurations at different reaction conditions. The theoretical studies by Bollinger et al. [42] have shown that it is important to take the adsorption of H into account when constructing such phase diagrams. The validity of these phase diagrams has been supported experimentally by STM images [45]. The phase diagrams, which includes the effect of hydrogen show that under typical HDS conditions the S edge ($\bar{1}$ 010) exposes S dimers, which are fully covered by adsorbed hydrogen (SH groups), whereas the Mo edge exposes S monomers, which are partly covered by adsorbed hydrogen [42,46].

In the present paper, we investigate poisoning effects using three different known inhibitors, i.e. benzene, pyridine and H₂S. DFT calculations have been performed on the interaction of these molecules with the Mo edge and the S edge of MoS₂ at S and H coverages, which are likely to be present under industrial HDS conditions. The effect of protonation of the basic pyridine molecule has also been investigated in order to elucidate the effect of Brønsted sites. The results provide insight into the nature of the HYD sites, the strong inhibition by pyridine and the weak inhibition of the HYD route by H₂S.

2. Calculation details

An infinite stripe model, which has previously proved suitable for providing insight into MoS₂, is used to investigate the edges of MoS₂, see Fig. 1 [41,42,47]. The edge configurations investigated in the present study can be seen in Fig. 2. The infinite stripe exposes both the Mo edge and the S edge. The supercell has four Mo atoms in the *x*-direction and four Mo atoms in the *y*-direction. The periodicity of four in the *x*-direction is necessary to allow for important reconstructions with a period of two. The dimension of the slab in the *y*-direction has been tested to be sufficient to decouple the Mo edge and the S edge in the *y*-direction. The stripes are separated by 14.8 Å in the *z*-direction and 9 Å in the *y*-direction in order to decouple the individual stripes. The basal plane of MoS₂ is investigated using a supercell with four Mo atoms in the *x*- and *y*-direction and a separation of 14.8 Å in the *z*-direction between individual MoS₂ slabs, see Fig. 1.

The plane wave density functional theory code *DACAP0* is used [48]. The Brillouin zone is sampled by three *k*-points in the *x*-direction and one *k*-point in the *y*- and *z*-direction for the stripe, and the three *k*-points in the *x*- and *y*-direction for the basal plane slab [49]. A plane-wave cutoff of 30 Rydberg is used and a density wave cutoff of 45 Rydberg is used, in order to improve the precision of the forces [50]. Ultrasoft pseudopotentials are used except for sulfur, where a soft pseudopotential has been used [51]. A Fermi temperature of

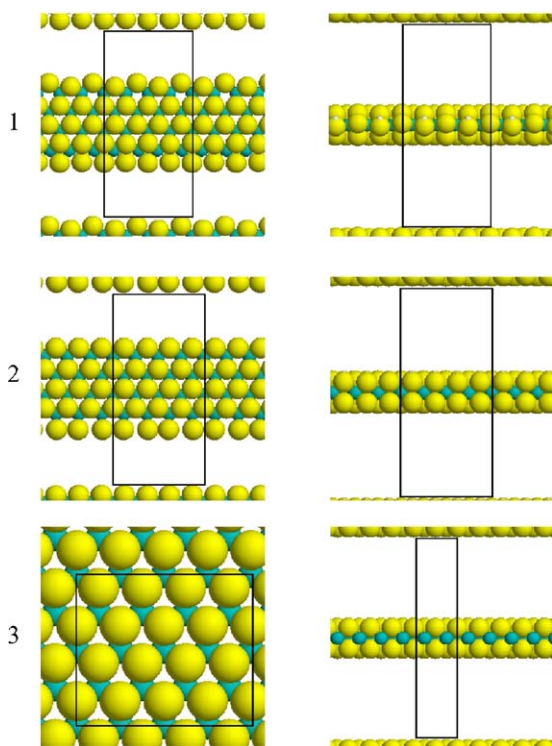


Fig. 1. Super cells used for studies on: (1) Mo edge; (2) S edge; (3) Basal Plane. Left side shows the top view and right side the side view. Color code: sulfur (yellow), molybdenum (green), hydrogen (white). For interpretation of the references to colour in this figure legend, the reader is referred to the web version of the article.

$k_B T = 0.1$ eV is used and all energies are extrapolated to zero electronic temperature. The exchange correlation functional PW91 has been used throughout the study [52]. The convergence criterion for the atomic relaxation is 0.15 eV/Å. The Nudge Elastic Bands (NEB) method is used to find energy barriers [53]. The adsorption energies are calculated using Eq. (1).

$$\Delta E_{\text{ad}} = (E_{\text{molecule/MoS}_2} - E_{\text{MoS}_2} - E_{\text{molecule(g)}}) \quad (1)$$

where $E_{\text{molecule/MoS}_2}$ is the energy of the system with the molecule bound to the surface, E_{MoS_2} the energy of the stripe/slab and $E_{\text{molecule(g)}}$ the energy of the free molecule. All energies are given at 0 K and do not include vibrational ground state energies. The lattice constant of MoS₂ is calculated to be $a = 3.215$ Å, which compares well with the experimental value of 3.16 Å. Figures have been made using Rasmol and VMD [54].

3. Results

3.1. Benzene

The adsorption of benzene has been investigated both at different regions along the Mo and the S edge and on the basal plane as a reference.

3.1.1. Mo edge

Benzene adsorption at the Mo edge has been investigated with a S coverage corresponding to HDS conditions and a H coverage of 25%. The H coverage chosen is below the 50% H coverage at equilibrium in order to investigate the influence of the distance between the adsorbed molecule and the H atom. The brim sites, which have been shown to be able to participate in hydrogenation [43] are positioned close to the front row S atoms and adsorption on these sites is also investigated. The investigated adsorption configurations at the Mo edge can be seen in Table 1. It is seen that the adsorption energy at the Mo edge is slightly exothermic and is similar for all configurations, while adsorption on the basal plane is thermoneutral as shown in configuration e in Table 1. The exchange correlation functional (XC-functional) used does not take van der Waals interactions into account and the difference in adsorption energies is therefore due to chemisorption. The change in

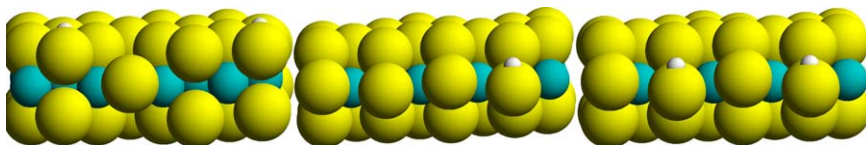


Fig. 2. Edge configurations investigated. Left is the S edge with a vacancy and 50% H coverage. Middle is the Mo edge with 50% S coverage and 25% H. Right is the Mo edge with 50% S coverage and 50% H.

Table 1
Benzene adsorption sites

	Configuration					
	a	b	c	d	e	f
H coverage [%]	25	25	25	25	–0.02	50
ΔE_{ad} [eV]	–0.14	–0.17	–0.16	–0.16	–0.02	0.02

Configurations a–d is at the Mo edge, configuration e is on the basal plane, and configuration f is at the S edge.

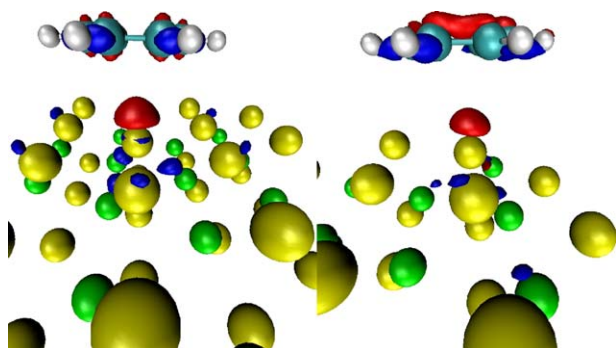


Fig. 3. Benzene electron-density difference plot. Left: Benzene on basal plane. Right: Benzene at Mo edge. Color code: Depletion of electron density (red) plotted at a contour value of $-0.003 \text{ e}^3/\text{\AA}$ increase in electron density (blue) plotted at a contour value of $0.003 \text{ e}^3/\text{\AA}$. For interpretation of the references to colour in this figure legend, the reader is referred to the web version of the article.

electron density can be seen in Fig. 3. The figure clearly shows that the changes in electron density upon adsorption are somewhat larger at the Mo edge than on the basal plane. Thus, there is a preference for the benzene molecule to adsorb at the Mo edge rather than on the basal plane. Furthermore, we have tested whether hydrogenation of benzene can stabilize the adsorption. We find that hydrogenation makes the adsorption energy endothermic.

3.1.2. S edge

Benzene adsorption at the S edge has been investigated with H and S coverages corresponding to HDS conditions and the S edge has been activated by the creation of a single vacancy. Benzene adsorption at the S edge has been investigated at a site next to the vacancy, as shown in configuration f Table 1. Only

one adsorption site has been investigated since the benzene adsorption energy is thermoneutral at the vacancy site and the Mo edge results indicated that small variation in the local structure at the adsorption site only lead to small changes in the adsorption energy. It is, therefore, presently assumed that the adsorption will not become more exothermic by moving the benzene molecule away from the vacancy. The adsorption energy at the S edge (configuration f) is similar to the adsorption energy on the basal plane (configuration e), indicating that there is no preference for the benzene to move from the Mo edge to the S edge. Thus, we can conclude that benzene does not adsorb at the S edge. This indicates that the S edge is not important for hydrogenation as benzene inhibits this reaction.

3.2. Pyridine and pyridinium

Adsorption of pyridine and the formation of pyridinium ion have been investigated at both the Mo edge and the S edge and as reference also on the basal plane.

3.2.1. Mo edge

Pyridine adsorption at the Mo edge has been investigated with S coverage corresponding to HDS conditions, i.e. 50% S coverage and with 25 or 50% H coverages. Formation of pyridinium has been investigated with 25% H coverage, which corresponds to moving a proton to the pyridine molecule and thereby lowering the edge coverage of H. The adsorption configurations of pyridine at the Mo edge (configurations a–h) and basal plane (configuration i) can be seen in Table 2. It is seen that the adsorption energies are slightly exothermic, and more exothermic than on the basal plane. Under HDS conditions, there is adsorbed hydrogen in form of SH groups in the vicinity of the pyridine. Therefore, one could imagine

Table 2
Pyridine and pyridinium ion adsorption sites

	Configuration					
	a	b	c	d	e	f
H coverage [%]	25	25	25	25	50	50
ΔE_{ad} [eV]	−0.12	−0.08	−0.09	−0.08	−0.09	−0.03
	Configuration					
	g	h	i	j	k	l
H coverage [%]	50	50	25	25	25	25
ΔE_{ad} [eV]	−0.01	−0.11	−0.03	−0.40	−0.45	−0.59

Configurations a–h is for pyridine at the Mo edge, configuration i is pyridine on the basal plane, and configurations j–k is the pyridinium ion at the Mo edge.

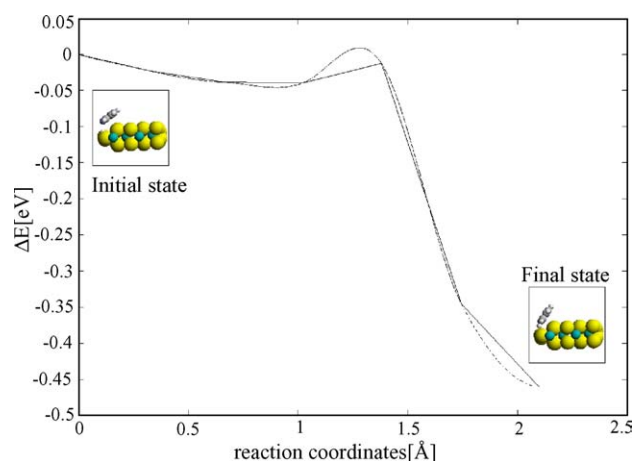


Fig. 4. The energy barrier for creating pyridium. The straight line connects the individual NEB Images and the curved line is splines fitted to the forces on the individual NEB images.

that a proton could be transferred from the neighboring SH group to the pyridine molecule, resulting in the formation of a pyridinium ion. Thus the formation of the pyridinium ion has also been investigated (configurations j–l in Table 2). The significant exothermic energies show that pyridinium ions are very stable at the Mo edge. The adsorption energies become approximately 0.4 eV more exothermic than for pyridine itself.

The barrier for the proton transfer has also been calculated and the results are shown in Fig. 4. The H transfer reaction is apparently non-activated, suggesting that pyridine will form pyridinium ions readily upon adsorption at the Mo edge. The electron density plots of pyridine and pyridinium ion adsorbed at the Mo edge and basal plane (Fig. 5) show a more pronounced change in the electron density when the adsorption occurs at the edge. The change in electron density is also significantly larger than for benzene (note that the contour value is a factor of 10 larger than the one used in the benzene density). It is also seen that as H^+ is transferred from the catalyst to pyridine, electron density is shifted to the catalyst, thus, indicating the formation of a pyridinium ion-like species.

3.2.2. S edge

Pyridine adsorption at the S edge has been investigated with H and S coverage corresponding to HDS conditions and as for the benzene study, the S edge has been activated by the creation of a single vacancy. Such a vacancy is likely to be involved in the DDS pathway and the present calculations, therefore, also allow us to get insight into poisoning effects on this route. The adsorption configurations are shown in configurations a–c in Table 3. Pyridine binds strongest when the N atom is positioned in the vacancy, as seen in configuration c and less strongly when the adsorption configurations are similar to those at the Mo

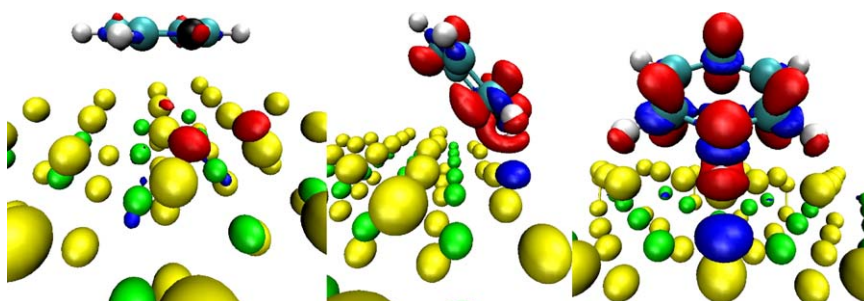


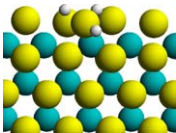
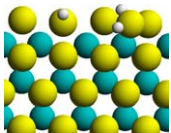
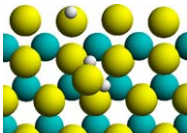
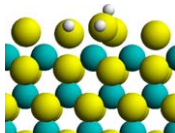
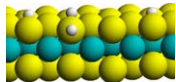
Fig. 5. Pyridine and pyridinium ion electron-density difference plot. Left: Pyridine on basal plane. Middle: Sideview of pyridinium ion at the Mo edge. Right: Frontview of pyridinium ion at the Mo edge. Color code: Depletion of electron density (red) plotted at a contour value of $-0.03 \text{ e}^3/\text{\AA}$ increase in electron density (blue) plotted at a contour value of $0.03 \text{ e}^3/\text{\AA}$. Nitrogen is black. For interpretation of the references to colour in this figure legend, the reader is referred to the web version of the article.

Table 3
S edge pyridine and pyridinium ion adsorption sites

	Configuration			
	a	b	c	d
Top view				
Front view				
H coverage [%]	25	25	25	25
ΔE_{ad} [eV]	−0.02	−0.05	−0.28	0.17

Configurations a–c is pyridine at the S edge with a vacancy and configuration d is the pyridinium ion at the S edge with a vacancy.

Table 4
H₂S adsorption sites at the Mo edge and the S edge

	Configuration				
	a	b	c	d	e
					
H coverage [%]	25	25	25	25	50
ΔE_{ad} [eV]	0.09	0.10	−0.06	−0.16	−0.12

Configurations a–d are at the Mo edge. Configuration e is a vacancy site at the S edge.

edge, as in configuration a and b. The observation that pyridine binds strongly to the vacancy is in agreement with the observation that the DDS route is poisoned by basic N compounds [13]. In configuration d, a H atom is added to the pyridine as shown in configuration a. This makes the adsorption endothermic. The adsorption at the S edge is less exothermic than at the Mo edge except for configuration c where pyridine is adsorbed in the vacancy. Pyridine in the vacancy is on the other hand less exothermic than the adsorption energies of pyridinium ions on the Mo edge (configuration j–l in Table 2). Therefore, the edge preference follows the same trend as for benzene adsorption, but the trend is more pronounced for pyridine. The reason why H does not stabilize pyridine as pyridinium at the S edge may be related to that the S edge S–H groups are less acidic than S–H groups at the Mo edge. This is reflected by a stronger binding energy at the S edge, 0.58 eV at the S edge compared to 0.37 eV at the Mo edge.

3.3. H₂S

H₂S is generally not considered to be a significant inhibitor for hydrogenation and, thus, it should adsorb much weaker than benzene and pyridine on the hydrogenation site. Studies of the H₂S adsorption, therefore, offer a way to supplement the above investigations. H₂S adsorption has, therefore, also been investigated at both the S and Mo edges.

3.3.1. Mo edge

H₂S adsorption at the Mo edge has been investigated with S coverage corresponding to HDS conditions and with a 25% H coverage. The lower than equilibrium H coverage is again chosen in order to investigate the influence of the distance between the adsorbed molecule and H. The adsorption configurations of H₂S at the Mo edge are shown in Table 4(a–d). Adsorption configuration d where H₂S is located next to the S–H group is found to be slightly exothermic (−0.16 eV), which is approximately the same adsorption energies as benzene at the Mo edge see Table 1. It should, however, be stressed that the van der Waals part of the adsorption energy for molecules with π systems is generally larger than for small molecules like H₂S. The adsorption of benzene and pyridine at the Mo edge is, therefore, expected to be stronger than H₂S.

3.3.2. S edge

H₂S adsorption at the S edge has been investigated at the S edge with H and S coverage corresponding to HDS conditions, where the S edge is again activated by the creation of one vacancy. The adsorption has been investigated at the vacancy as shown in configuration e in Table 4. The adsorption energy is seen to be exothermic (−0.12 eV), which is similar to that on the Mo edge. The adsorption of H₂S is, therefore, equally likely at both edges. Dissociation of H₂S is not considered in this study but has been found elsewhere to be highly exothermic (−1.6 eV). This result explains the strong inhibition of the DDS pathway by H₂S [55].

4. Discussion

One of the main reasons why it has been difficult to understand the reactivity and inhibition effects observed under deep HDS can be related to the fact that very little information has been available regarding the HYD pathway, which plays an important role under such conditions [5,7–9,11,13,14,16,18]. The fact that large sterically hindered alkyl substituted molecules like 4,6-DMDBT can react via the HYD route has led researchers to propose that multiple vacancies are involved in the reaction via an initial π bonding of the reactants [35,56]. This proposal can rationalize several observations but it has not allowed one to understand several observations including the large difference in the inhibition effects between molecules such as benzene and pyridine. Also, the absence of a strong inhibition effect by H₂S has been difficult to understand using the above proposal for the HYD sites, since one might expect that such sites would have a large affinity toward sulfur. Indeed, recent DFT results [41,42] have shown that such vacancy sites bind sulfur strongly again suggesting that other sites may be involved. For a long time, the nature of such sites remained unclear but recently STM and DFT results revealed that quite different sites might be involved in HYD, namely, the metallic like brim sites located adjacent to the edges [42,43,45,57]. It was proposed that the involvement of such sites might also be consistent with the different observed inhibition effects [58]. The present results have confirmed this and have provided detailed insight into the nature of the inhibiting effects.

It is, presently, observed that the availability of hydrogen at the catalyst surface plays an essential role in the poisoning by

basic nitrogen compounds like pyridine. Hydrogen reacts with pyridine and forms the pyridinium ion and this stabilizes its adsorption. This process is favored at the Mo edge. Pyridinium ions were previously observed in IR experiments [30] and our present findings substantiate the proposal that S–H groups are involved in the pyridinium ion formation. It is interesting that the present results show that the formation of pyridinium ions is expected to occur predominantly at the Mo edge. Without the formation of pyridinium ions benzene would have been a stronger inhibitor than pyridine because it is seen to bind stronger. However, due to the influence of hydrogen, pyridine is a much stronger poison. In this context, it is important that hydrogen binds less strongly at the Mo edge (but it still binds) as compared to the S edge. Actually, at the Mo edge, hydrogen is bound almost with zero free energy [46] and, therefore, can be easily transferred to the pyridine molecule. It is also likely that the weakly bound H atoms at the Mo edge could be important in hydrogenation reactions at the Mo edge.

Benzene is found to be less strongly bound than the pyridinium ion, and this explains why benzene is less poisonous than pyridine. Both benzene and pyridine/pyridinium ion preferably adsorb at the Mo edge indicating that the active site for hydrogenation is located at the Mo edge. The adsorption study of H₂S substantiates that the hydrogenation site is at the Mo edge, since H₂S adsorbs weakly here in agreement with the very weak poisoning of the HYD pathway. This result confirms STM and DFT results showing that the hydrogenation occurs at regions close to the Mo edge (the brim sites) [43]. Inhibition of hydrogenation reactions by pyridine is not only due to blocking, since when it is protonated it also uses H from the Brønsted acid sites, thereby, reducing the number of H atoms available for hydrogenation.

The observation that heavier molecules, like quinolines and acridines are stronger poisons than pyridine [20,21], can be explained by two effects. Firstly, the van der Waals interaction increases for molecules with more π systems. This increase in van der Waals interaction can probably be assumed to be quite independent of the nature of the adsorption site, meaning that the adsorption energy would also increase similarly for all sites. The second and probably more important effect is that the inhibition by basic nitrogen compounds increases with higher proton affinity as found in experimental studies [20,21]. The present study has shown that there is no significant barrier for proton transfer from the S–H groups to pyridine at the Mo edge and if one assumes that this is also the case for larger molecules than pyridine, then the proton transfer will only be equilibrium limited. It is, therefore, reasonable to expect that the gas phase proton affinity correlate quite well with the inhibitor strength because a similar proton transfer process is taking place on the catalyst.

While the present investigation has mainly focused on the poisoning of the HYD pathway several of the results also provide insight into the poisoning of the DDS pathway. For example, it is seen that pyridine adsorbs quite strongly in a vacancy site at the S edge. This may be the origin of the poisoning effects by N compounds of the DDS pathway, which

dominates for the HDS reaction of rather reactive sulphur compounds like DBT [13].

Promoted catalysts have not been studied, presently, but the present results allow a basis for understanding certain inhibition effects in such catalysts. For Co promoted catalyst, the promoter prefers to be located at the S edge resulting in the formation of the CoMoS phase [13,41,44,57]. This results in the creation of new sites, which may interact with inhibitors. Mo edges will, however, also be present and they will resemble those in unpromoted catalysts. The present results may, thus, provide a starting point for understanding promoted catalysts.

5. Conclusion

In order to develop new catalysts, which can meet the increasing demands for the production of ultra low sulfur transportation fuels, it is necessary to understand in detail the reaction involved in the removal of sterically hindered sulfur containing molecules and how other molecules in the feed may inhibit these reactions. The present results have provided new insight in this regard. It is seen that the poisoning of the important HYD route occurs quite differently from the most commonly accepted proposals in the literature. For example, it is seen that the inhibiting effect by aromatics is not due to the interactions with highly uncoordinated vacancies (like the naked Mo edges) but rather with the fully coordinated molybdenum sites like the metallic-like brim sites located adjacent to the edge itself. The π -bonding to such sites explains the poisoning by aromatics. This bonding is not much affected by substituents in DBT and this explains why the HYD route is more favored for refractory molecules than the DDS route. The present results show that the fully coordinated brim sites bind H₂S very weakly. Thus, the lack of significant inhibition by H₂S, which has intrigued researchers for decades, can readily be explained. The strong poisoning by pyridine is observed to be due to an increase in adsorption energy upon protonation of the pyridine molecule. The proton donor is a neighboring S–H Brønsted acid site located at the Mo edge. The pyridine to pyridinium ion reaction is found to be non-activated. Both benzene and pyridine prefers to adsorb at the Mo edge and both acts as poison for the hydrogenation pathway, which support the conclusion that the hydrogenation site is located at the Mo edge. The present results also show that pyridine will poison vacancy sites involved in the direct desulfurization path. In this case, the poisoning occurs via direct coordination and without pyridinium ion formation.

In the future, the present studies should be extended to include promoted systems, support interactions, and other active phase modifications. DFT studies of the HDN reaction like those in [59,60] may also provide insight relevant for understanding the inhibition by nitrogen compounds. Recently, DFT calculations have shown that changes in support interactions influence the binding properties of MoS₂-based structures [47]. In fact, such changes may influence the hydrogenation sites, the binding of hydrogen and the apparent acidity of the hydrogen. Thus, support effects are also expected to influence the inhibition by different molecules and the

present type studies may provide a better basis for understanding and controlling the effect of inhibitors.

Acknowledgements

Fruitful discussions with Per Zeuthen and Duayne Whitehurst are gratefully acknowledged. We acknowledge support from the Danish center for scientific computing through grant number HDW-1101-05.

References

- [1] M. Houalla, N.K. Nag, A.V. Sapre, D.H. Broderick, B.C. Gates, *AIChE J.* 24 (1978) 1015.
- [2] M. Houalla, D.H. Broderick, A.V. Sapre, N.K. Nag, V.H.J. de Beer, B.C. Gates, H. Kwart, *J. Catal.* 61 (1980) 523.
- [3] A. Amorelli, Y.D. Amos, C.P. Halsig, J.J. Kosman, R.R.J. Jonke, M. DeWind, J. Vrieling, *Hydrocarb. Process.* 71 (1992) 93.
- [4] I. Mochida, K. Sakanishi, X. Ma, S. Nagao, T. Isoda, *Catal. Today* 29 (1996) 185.
- [5] X. Ma, K. Sakanishi, I. Mochida, *Ind. Eng. Chem. Res.* 35 (1996) 2487.
- [6] M.V. Landau, *Catal. Today* 36 (1997) 393.
- [7] B.C. Gates, H. Topsøe, *Polyhedron* 16 (1997) 3213.
- [8] D.D. Whitehurst, T. Isoda, I. Mochida, *Adv. Catal.* 42 (1998) 345.
- [9] K.G. Knudsen, B.H. Cooper, H. Topsøe, *Appl. Catal. A* 189 (1999) 205.
- [10] H. Schulz, W. Bohringer, P. Waller, F. Ousmanov, *Catal. Today* 49 (1999) 87.
- [11] C. Song, *Catal. Today* 86 (2003) 211.
- [12] T.C. Ho, *Catal. Today* 98 (2004) 3.
- [13] H. Topsøe, B.S. Clausen, F.E. Massoth, *Hydrotreating catalysis*, in: J.R. Anderson, M. Boudart (Eds.), *Science and Technology*, vol. 11, Springer-Verlag, Berlin, New York, 1996.
- [14] T. Kabe, A. Ishihara, H. Tajima, *Ind. Eng. Chem. Res.* 31 (1992) 1577.
- [15] V. Meille, E. Schulz, M. Lemaire, M. Vrinat, *J. Catal.* 170 (1997) 29.
- [16] M. Egorova, R. Prins, *J. Catal.* 225 (2004) 417.
- [17] F. van Looij, P. van der Laan, W.H.J. Stork, D.J. Di Camillo, J. Swain, *Appl. Catal. A* 170 (1998) 1.
- [18] M. Breyse, G. Djega-Maridassou, S. Pessayre, C. Geantet, M. Vrinat, G. Perot, M. Lemarie, *Catal. Today* 84 (2003) 129.
- [19] M. Nagai, T. Kabe, *J. Catal.* 81 (1983) 440.
- [20] M. Nagai, T. Sato, A. Aiba, *J. Catal.* 97 (1986) 52.
- [21] V. LaVopa, C.N. Satterfield, *J. Catal.* 110 (1988) 375.
- [22] P. Zeuthen, K.G. Knudsen, D.D. Whitehurst, *Catal. Today* 65 (2001) 307.
- [23] P. Wiwel, K.G. Knudsen, P. Zeuthen, D.D. Whitehurst, *Ind. Eng. Chem. Res.* 39 (2002) 533.
- [24] M. Egorova, R. Prins, *J. Catal.* 224 (2004) 278.
- [25] E. Furimsky, F.E. Massoth, *Catal. Today* 52 (1999) 381.
- [26] T.C. Ho, *J. Catal.* 219 (2003) 442.
- [27] U.T. Turaga, X. Ma, C. Song, *Catal. Today* 86 (2003) 265.
- [28] M. Egorova, R. Prins, *J. Catal.* 221 (2004) 11.
- [29] N.-Y. Topsøe, H. Topsøe, *J. Catal.* 139 (1993) 641.
- [30] N.-Y. Topsøe, H. Topsøe, F.E. Massoth, *J. Catal.* 119 (1989) 252.
- [31] X.L. Ma, K. Sakanishi, I. Mochida, *Ind. Eng. Chem. Res.* 34 (1995) 748.
- [32] E.A. Blekkan, A. Virnovskaia, H. Bergen, P. Steiner, *ACS Fuel Chem. Div. Prepr.* 48 (2003) 37.
- [33] T. Kabe, W. Qian, A. Ishihara, *Catal. Today* 39 (1997) 2.
- [34] J. Miciukiewicz, W. Zmierczak, F.E. Massoth, in: *Proceedings of the Eighth International Conference of Catal.* Verlag Chemie, Berlin, 1984, p. 671.
- [35] X.L. Ma, H.H. Schobert, *ACS. Div. Petrol. Chem. Prepr.* 213 (1997) 15.
- [36] S. Cristol, J.F. Paul, E. Payen, D. Bougeard, F. Hutschka, S. Clemendot, *J. Catal.* 224 (2004) 138.
- [37] P. Raybaud, J. Hafner, G. Kresse, H. Touilhoat, in: B. Delmon, G.F. Froment, P. Grange (Eds.), *Hydrotreatment and Hydrocracking of Oil Fractions*, Elsevier, 1999, p. 309.
- [38] P. Raybaud, J. Hafner, G. Kresse, H. Toulhaut, *Phys. Rev. Lett.* 80 (1998) 1481.
- [39] H. Yang, C. Fairbridge, Z. Ring, *Energy Fuels* 17 (1993) 387.
- [40] H. Orita, K. Uchida, N. Itoh, *J. Mol. Catal. A* 193 (2003) 197.
- [41] L.S. Byskov, J.K. Nørskov, B.S. Clausen, H. Topsøe, *J. Catal.* 187 (1999) 109.
- [42] M.V. Bollinger, K.W. Jacobsen, J.K. Nørskov, *Phys. Rev. B* 67 (2003) 085410.
- [43] J.V. Lauritsen, M. Nyberg, J.K. Nørskov, B.S. Clausen, H. Topsøe, E. Lægsgaard, F. Besenbacher, *J. Catal.* 224 (2004) 94.
- [44] H. Schweiger, P. Raybaud, H. Toulhaut, *J. Catal.* 212 (2002) 33.
- [45] J.V. Lauritsen, M.V. Bollinger, E. Lægsgaard, K.W. Jacobsen, J.K. Nørskov, B.S. Clausen, H. Topsøe, F. Besenbacher, *J. Catal.* 221 (2004) 510.
- [46] B. Hinnemann, P.G. Moses, J. Bonde, K.P. Jørgensen, J.H. Nielsen, S. Horch, I. Chorkendorff, J.K. Nørskov, *J. Am. Chem. Soc.* 127 (15) (2005) 5308.
- [47] B. Hinnemann, J.K. Nørskov, H. Topsøe, *J. Phys. Chem. B* 109 (6) (2005) 2245.
- [48] www.camp.dtu.dk/campos/.
- [49] H.J. Monkhorst, J.D. Pack, *Phys. Rev. B* 13 (1976) 5188.
- [50] K. Laasonen, A. Pasquarello, R. Car, C. Lee, D. Vanderbilt, *Phys. Rev. B* 47 (1993) 10142.
- [51] D. Vanderbilt, *Phys. Rev. B* 41 (1990) 7892.
- [52] J.P. Perdew, J.A. Chevary, S.H. Vosko, K.A. Jackson, M.R. Pederson, D.J. Singh, C. Fiolhais, *Phys. Rev. B* 46 (11) (1992) 6671.
- [53] H. Jonsson, G. Mills, K.W. Jacobsen, in: B.J. Berne, G. Cicotti, D.F. Coker (Eds.), *Classical and Quantum Dynamics in Condensed Phase Systems*, World Scientific, 1998.
- [54] W. Humphrey, A. Dalke, K. Schulten, *J. Mol. Graphics* 14 (1996) 33–38.
- [55] P.G. Moses, Unpublished results.
- [56] X. Ma, H.H. Schobert, *J. Mol. Cat. A* 160 (2000) 409.
- [57] J.V. Lauritsen, S. Helveg, M. Nyberg, E. Lægsgaard, I. Stensgaard, B.S. Clausen, H. Topsøe, F. Besenbacher, *J. Catal.* 197 (2001) 1.
- [58] H. Topsøe, B. Hinnemann, J.K. Nørskov, J.V. Lauritsen, F. Besenbacher, P.L. Hansen, G. Hyltoft, R.G. Egeberg, K.G. Knudsen, *Catal. Today* 107–108 (2005) 12.
- [59] M. Sun, A.E. Nelson, J. Adjaye, *J. Mol. Catal. A* 222 (2004) 243.
- [60] M. Sun, A.E. Nelson, J. Adjaye, *J. Catal.* 231 (2005) 223.